

# Magmatic lineations inferred from anisotropy of magnetic susceptibility fabrics in Units 8, 9, and 10 of the Rum Eastern Layered Series, NW Scotland

B. O'Driscoll <sup>a,\*</sup>, R.B. Hargraves <sup>b,1</sup>, C.H. Emeleus <sup>c</sup>, V.R. Troll <sup>a</sup>,  
C.H. Donaldson <sup>d</sup>, R.J. Reavy <sup>e</sup>

<sup>a</sup> Department of Geology, Museum Building, Trinity College, Dublin 2, Ireland

<sup>b</sup> Formerly of the Geosciences Faculty, Princeton University, NJ 08542, USA

<sup>c</sup> Department of Earth Sciences, University of Durham, Science Laboratories, South Road, Durham, DH1 3LE, UK

<sup>d</sup> School of Geography and Geosciences, University of St. Andrews, St Andrews, Fife, KY16 9AL, UK

<sup>e</sup> Department of Geology, University College Cork, Cork, Ireland

Received 4 March 2006; accepted 26 January 2007

Available online 2 February 2007

## Abstract

The Eastern Layered Series of the Rum Layered Suite, NW Scotland, comprises a sequence of sixteen (30–150 m thick) cyclic units. The upper troctolite–olivine gabbro parts of each of these units exhibit small-scale modal layering and a pervasive, layer-parallel mineral lamination that is often associated with ‘soft-sediment’ deformation structures. A sporadic, macroscopic magmatic lineation measurable on mineral lamination surfaces is also observed in places. Anisotropy of magnetic susceptibility (AMS) fabrics were studied in three of these cyclic units, (8, 9, and 10) in the northern part of the Eastern Layered Series. Magnetic fabrics measured in the troctolites and gabbros yield one dominant trend in which magnetic foliations parallel magmatic layering and magnetic lineations trend NW–SE and plunge gently. Magnetic fabrics measured for two detailed traverses through Unit 10 on the northern side of Hallival also yield one dominant trend, similar to that measured elsewhere in the Eastern Layered Series. However, toward the centre of Unit 10 in each traverse, magnetic lineations sometimes plunge approximately downdip (SW) on the magnetic foliation planes. The implications of these results are discussed with reference to previous textural and fabric observations on Rum. A model is suggested in which weak linear arrangements of cumulus olivine and plagioclase crystals are developed due to slumping and soft-sediment deformation of unconsolidated crystal mushes during central sagging of the Rum Layered Suite.

© 2007 Elsevier B.V. All rights reserved.

**Keywords:** Rum Eastern Layered Series; Anisotropy of magnetic susceptibility; Modal layering; Mineral lamination; Central sagging

\* Corresponding author. Present address: School of Geological Sciences, University College Dublin, Belfield, Dublin 4, Ireland. Tel.: +353 17162326.

E-mail address: [brian.odriscoll@ucd.ie](mailto:brian.odriscoll@ucd.ie) (B. O'Driscoll).

<sup>1</sup> This work is dedicated to the memory of R.B. Hargraves, who initiated this work on AMS fabrics in the Eastern Layered Series of Rum, before his death in March 2003.

## 1. Introduction

Considerable controversy surrounds the development of magmatic layering and associated planar crystal arrangements (mineral lamination) observed in many mafic to ultramafic intrusions (see [Irvine et al., 1998](#) for

review). In addition to the classic cumulus theory of Wager and Brown (1968) that attributes layering to crystal settling and magmatic sedimentation processes, an extensive array of models, including monomineralic phase-precipitation, melt migration due to compaction, and *in situ* crystallisation, have also been held responsible (e.g. Jackson, 1961; McBirney and Noyes, 1979; Meurer and Boudreau, 1998). Even in cases where layering and mineral lamination are exceptionally well developed, it is generally difficult to unequivocally attribute layer development to any one model. In the Rum layered intrusion, and in many others, a host of post-cumulus processes are believed to have significantly modified the primary composition and textures of layered rocks at a variety of scales (Butcher et al., 1985; Young et al., 1988; Emeleus et al., 1996; Holness, 2005). These include compaction, melt migration, channelled metasomatism, and textural re-equilibration. It is often difficult to distinguish between the contributions of primary and secondary (postcumulus) processes to magmatic layering and igneous fabric development in sequences of layered rocks. Indeed, in the absence of macroscopic linear arrangements of crystals (magmatic lineations) or sedimentary structures (scour structures or cross bedding), differentiating even between primary processes such as magmatic sedimentation or *in situ* crystallisation may prove extremely challenging.

Measurements of the anisotropy of magnetic susceptibility (AMS) of igneous rocks can determine the preferred orientation of the magnetic minerals in a sample even when visible mineral alignment fabrics are weak or absent (Hargraves et al., 1991; Rochette et al., 1992; Tarling and Hrouda, 1993; Bouchez, 1997). Though the technique has advanced understanding of magma flow in dykes and lava flows of varying composition as well as in intrusive granitoids, there is comparatively little AMS work reported in the literature on large layered, mafic to ultramafic intrusions (e.g. Bolle et al., 2000, 2002; Ferré et al., 2002). Despite the long-standing problems with interpreting the AMS in rocks where there may be different magnetic carriers, the technique is a useful tool in the study of fabrics in layered rocks as it potentially reveals the shape, strength and orientation of the magnetic fabric in a sample; quantities that are often not evident from field or thin-section analyses of silicate fabrics.

The Rum Layered Suite occurs in one of the igneous centres of the British Palaeogene Igneous Province (developed during the opening of the North Atlantic) and is a well-exposed example of a layered, mafic–ultramafic intrusion (Emeleus, 1987; Emeleus et al., 1996; Emeleus and Bell, 2005). This article focuses on

the relationship between magmatic layering (and associated structures) and AMS fabrics in three layered units in the northern part of the well-studied Eastern Layered Series of the Rum Layered Suite. Building on grain orientation measurements carried out by Brothers (1964), we combine our field observations and those of other workers with AMS data to evaluate the processes involved in formation of the observed layering and fabrics in the Rum cumulate pile.

## 2. Geological setting

The Isle of Rum is one of the Inner Hebridean ‘Small Isles’, located off the NW Scottish coast. The Layered Suite of the Palaeogene Rum Central Complex forms an upstanding area of about 30 km<sup>2</sup> in the central and eastern parts of the island. The suite has been divided into three as follows: the Eastern Layered Series, Western Layered Series, and the Central Series (Fig. 1). Age relations between the Eastern Layered Series and the Western Layered Series are uncertain; although the Western Layered Series is a structurally lower part of the intrusion, it is separated from the Eastern Layered Series by the younger Central Series (Emeleus et al., 1996). The subject of this study, the Eastern Layered Series (Fig. 1a and b), comprises a sequence of peridotite–troctolite cyclic macro-units, in which peridotite is always overlain by modally layered troctolite (historically termed allivalite) and in some cases, olivine gabbro (e.g. Units 9 and 10). The peridotite bases of units are generally sharp, and are occasionally marked by thin chrome–spinel seams (e.g. Units 6/7, 7/8 and 11/12; Brown, 1956). The exposed sequence of the Eastern Layered Series has been divided into sixteen such units (Brown, 1956; Volker and Upton, 1990; Emeleus et al., 1996), whose thicknesses range from a few tens of metres to ~100 m (Fig. 1). This stratigraphy has been shown to be overly simplistic by Bédard et al. (1988) and Holness (2005) who present strong evidence that the Unit 9 peridotite is a late, layer-parallel intrusive body. However, Holness (2005) has also demonstrated that Unit 9 is probably the only major intrusive peridotite body in the Eastern Layered Series.

The cyclic units of the Eastern Layered Series dip towards a focus at a point along the Long Loch Fault, a major north–south trending structure that bisects the island (Fig. 1c), and that is believed to be the principal conduit for the Rum Layered Suite magmas (Emeleus et al., 1996). Dips are generally 10°–15° but may locally be as much as 40° or more (Volker and Upton, 1990). The large-scale layering of the Eastern Layered Series is thought to have developed through replenishment of a

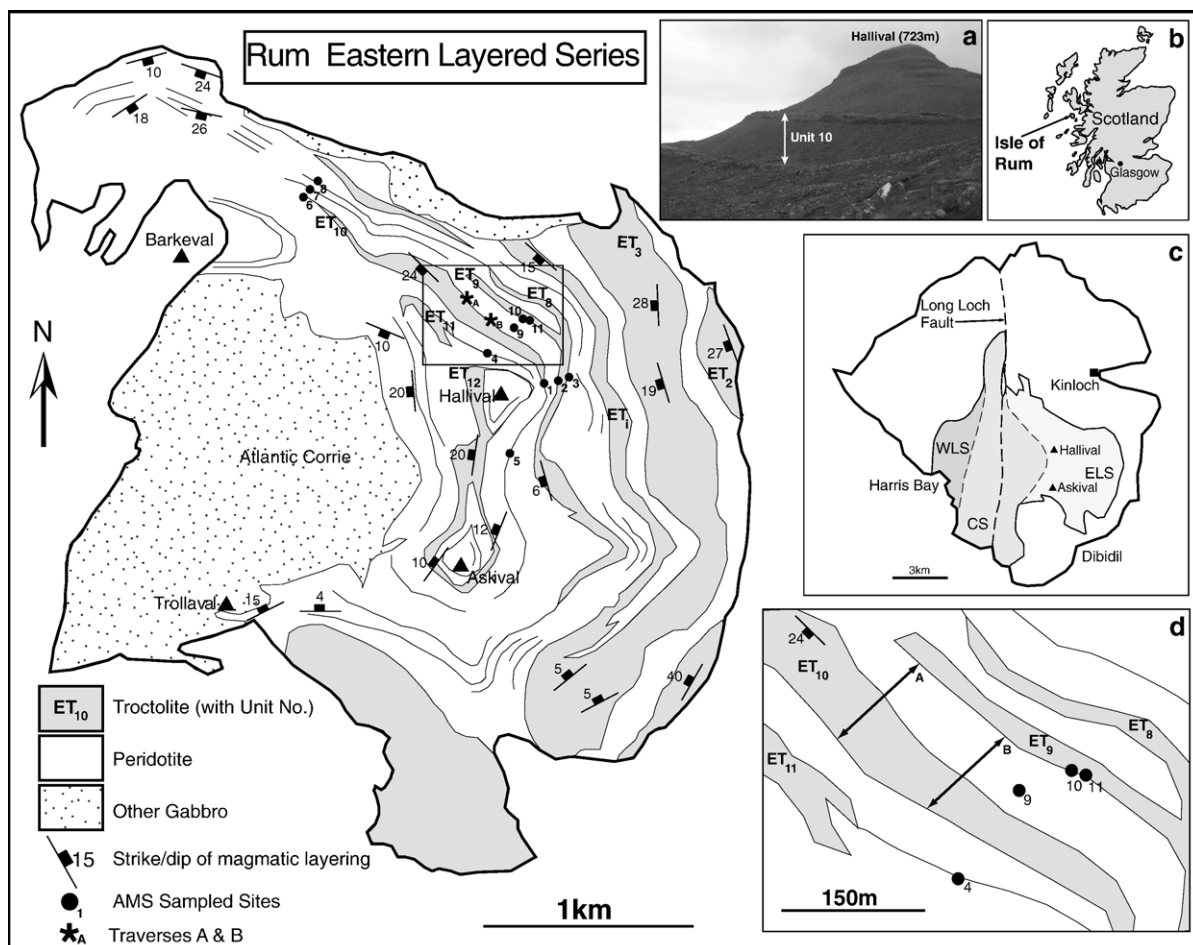


Fig. 1. Map of the Eastern Layered Series in the Rum Layered Suite, AMS sampling localities, and structural data measured from large-scale magmatic layering (the latter after [Emeleus et al., 1996](#)). (a) Northern slopes of Hallival, the resistant pale rock steps are the upper troctolite parts of each Unit, and the intervening slack ground the lower peridotites. (b) Schematic map of Scotland showing the location of the Isle of Rum in the Inner Hebrides. (c) Schematic map of the Isle of Rum showing the positions of the Eastern, Western and Central Layered Series (ELS, WLS and CS, respectively). (d) Enlarged map of the area highlighted in the main map of the Eastern Layered Series showing the positions of the detailed traverses carried out on the northern slopes of Hallival.

magma chamber by picritic magmas that ponded in thin sill-like bodies, each contributing incrementally to the layered sequence ([Emeleus et al., 1996](#)). These authors envisaged emplacement of each of these units as major pulses of magma spreading out across the floor of a ‘persistently reconstituted, thin, sill-like magma chamber’. Furthermore, they suggest that the body of magma in the intrusion at any given time may have been no more than several tens to hundreds of metres thick.

Early work carried out on the cumulate rocks of the Rum Eastern Layered Series employed a classic fractionation model, involving crystal settling of successive crops of minerals from a replenishing mafic magma ([Brown, 1956](#); [Dunham and Wadsworth, 1978](#)).

Initial crystallisation and separation of chromite and olivine from each new batch of magma was followed by plagioclase and clinopyroxene, resulting in a cumulate stratigraphy that passed from peridotite at the base to troctolite and in several cases, olivine gabbro, at the top of each cyclic unit. More recent studies have elaborated on this model, and also highlighted the importance of a number of other magma chamber processes in the development of the Eastern Layered Series cumulates. For example, microanalytical and quantitative textural studies led [Worrell \(2002\)](#) and [Tepley and Davidson \(2003\)](#) to suggest that large-scale gravity-driven plumes were effective in transporting and mixing of crystal populations grown elsewhere in the magma chamber.

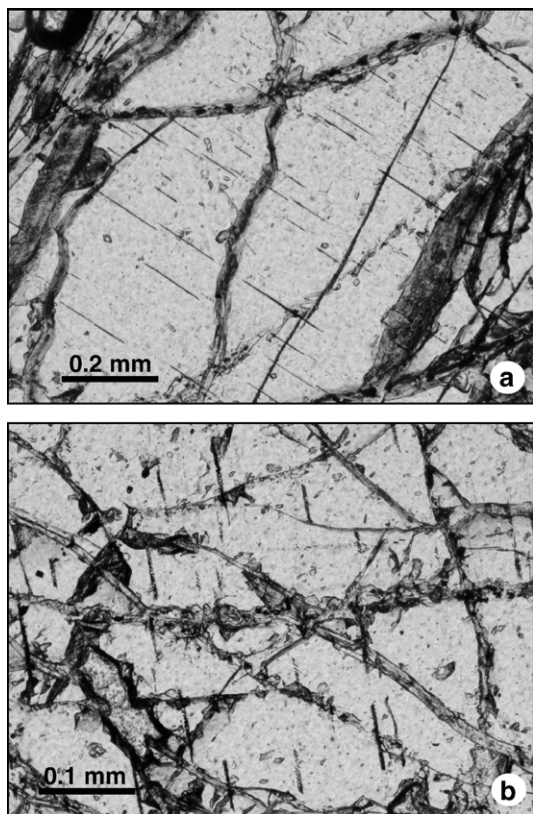


Fig. 2. (a and b) Photomicrographs of two examples of magnetite platelets in olivine crystals from the Unit 10 troctolite, illustrating the strong crystallographic control that olivine exerts on platelet orientation. In (a), the platelets trend NW–SE across the image, and in (b) they trend approximately N–S. Networks of veins that traverse olivine crystals are typically infilled with serpentine.

Some work has also focused on the importance of the intrusion of peridotite into the crystal mush pile instead of at the crystal mush–magma interface (Butcher et al., 1985; Bédard et al., 1988; Volker and Upton, 1991; Holness, 2005), and the postcumulus effects on the crystal mush of mobile and aggressive intercumulus liquids (Holness, 2005). Renner and Palacz (1987) and O'Driscoll et al. (2007) also note the importance of frequent minor influxes of melt into the Rum cumulates, referring to the Rum magma chamber as a 'leaky' open system.

A substantial body of evidence exists for centrally directed sagging of the cyclic units of the Rum Layered Suite toward a point on the Long Loch Fault directly to the west of the Atlantic Corrie area (Fig. 1). This includes steepening of dips of layering at all scales (e.g. at least 40° in the Trollaval region; Volker and Upton, 1990) toward the Long Loch Fault and an abundance of soft-sediment deformation structures as outlined in

Section 3. It is unlikely that this deformation took place during emplacement of a cyclic unit, rather shortly afterward, so that following initial emplacement, each unit began to undergo sagging as it cooled (Emeleus et al., 1996). The latter authors also suggest that episodes of magma withdrawal and deflation along the Long Loch Fault were the mechanisms responsible for this central sagging.

### 3. Petrology of the Eastern Layered Series rocks

#### 3.1. Mineralogy

The peridotite portion of each Eastern Layered Series cyclic unit contains up to 80% subhedral olivine grains, with subsidiary equant chromite grains, and minor interstitial plagioclase and clinopyroxene, whereas the troctolite contains up to 70% subhedral plagioclase grains, with olivine and chromite. The olivine gabbro present at the tops of some units contains approximately equal amounts of subhedral clinopyroxene and plagioclase, with up to 15% olivine. In addition, each lithology contains varying amounts of hydrous minerals, (e.g. hornblende, phlogopite and serpentine), as well as a variety of oxides and sulphides (Housden et al., 1996). However, the significant variation in olivine content of the peridotite and troctolite parts of each unit means that different concentrations of iron existed in each lithology that might contribute to magnetic mineral formation after solidification. This led Housden et al. (1996) to suggest that "in some way the non-magnetic silicate mineralogy controlled the operation of processes responsible for the magnetic mineral formation".

The Eastern Layered Series magmas did not evolve sufficiently to crystallise cumulus magnetite; the only primary magnetic minerals that crystallised are chromite and very minor magmatic sulphide phases (Brown, 1956; Emeleus et al., 1996; Housden et al., 1996; Butcher et al., 1999). Housden et al. (1996) note that chromite typically occurs as both sub-equant intercumulus grains, up to 0.2 mm in size and also as early-formed rounded inclusions, (0.05–0.1 mm) within cumulus olivine in Unit 10. Typical sulphides (pentlandite, chalcopyrite, millerite) occur as composite interstitial grains approximately 50 µm in size, and are commonly associated with haematite in the peridotite portion of Unit 10. Housden et al. (1996) found that sulphide grains within the troctolite are mostly pyrrhotite, and are not associated with oxide minerals, concluding that the troctolites at the top of the unit are significantly less oxidized.

In their detailed petrographic study of the magnetic mineralogy of Unit 10, Housden et al. (1996) found that in

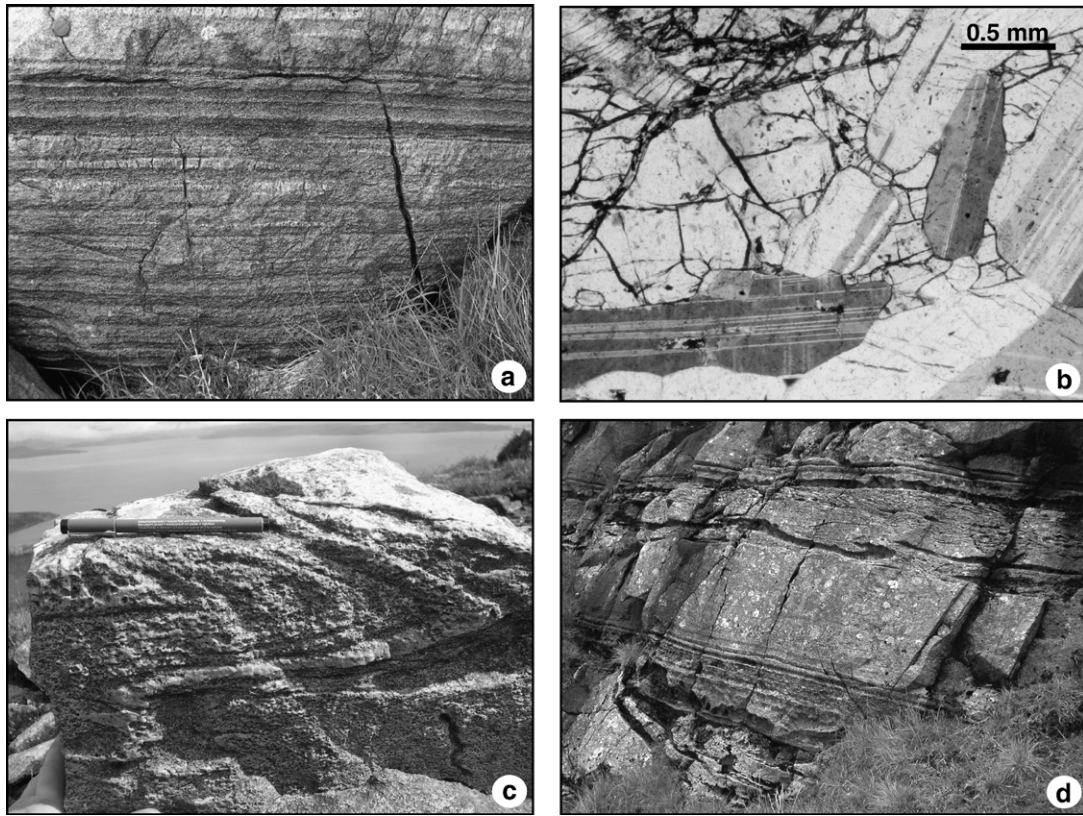


Fig. 3. (a) Small-scale magmatic layering of peridotite and troctolite from the upper part of Unit 10, northern face of Hallival (lens cap in upper left of photo is 4 cm in diameter). (b) Photomicrograph illustrating plagioclase crystals draping around an olivine grain in a troctolite from Unit 9. (c) Slump fold in layered troctolite from Unit 11, northern face of Hallival (pen in top left of image is 14 cm in length). (d) Flame structures in a sequence of troctolite layers, southern side of Hallival (layered sequence is ~4 m thick).

addition to the intra-olivine chromites, Fe–Ti oxides and sulphides, rectangular plate-like opaque inclusions are very frequently observed in olivine grains in both the peridotites and the troctolites. These occur in a range of sizes (10–400  $\mu\text{m}$  in length), though lengths of 30–50  $\mu\text{m}$  are most common (see Fig. 2a and b). Housden et al. (1996) described two platelet types; ‘homogenous’ and ‘dendritic’, and noted that both lie with their edges parallel to the crystallographic axes of the host olivine, i.e. have ‘a strong alignment parallel to the olivine *c*-axis’. The homogenous platelets tend to be of a uniform massive appearance, whereas the dendritic platelets are not uniform over their surface area. All platelets tend to be concentrated away from the edges of the olivine crystals, a fact that led Moseley (1984) to suggest that they formed through exsolution during cooling of the olivine. An electron microprobe traverse across a dendritic platelet edge carried out by Housden et al. (1996) revealed increases in Fe, Ca, Cr, Al and Ti and decreases in Si and Mg relative to the olivine host, an observation they attributed to the presence of two phases in the inclusions, one rich in

Si, Mg and Ca (clinopyroxene), and one rich in Fe, Cr and Ti (magnetite). The observations of Housden et al. (1996) supported the evidence already presented by Putnis (1979) and Moseley (1984) that the opaque platelets in olivine in the Eastern Layered Series were principally composed of intergrown magnetite and clinopyroxene. In addition, Moseley’s (1984) detailed crystallographic study on an olivine grain sampled from Unit 10 had shown that the direction in the magnetite at right angles to (110) is parallel to the direction at right angles to (001) of the olivine, consistent with the observation of Housden et al. (1996) in this regard. Housden et al. (1996) demonstrate that, with increasing height in Unit 10, platelets become more abundant in olivines, as well as becoming larger and more branching. They also note that well-formed dendritic platelets are only present in the troctolites. The palaeomagnetic study of Dagley and Musset (1981) found that near-pure magnetite is the only ubiquitous ferromagnetic mineral present in the Rum Layered Suite, and the sole carrier of remanent magnetism.

### 3.2. Petrofabrics and small-scale deformation structures associated with layering

Layering on the scale of millimetres to tens of centimetres is commonly observed within units of the Eastern Layered Series (Brown, 1956; Fig. 3a). In particular, the upper troctolitic sections of each unit are

associated with small-scale modal layering, resulting from numerous mm- to cm-thick peridotite layers interleaved with troctolite. This peridotite is mineralogically and texturally similar in appearance to the much thicker peridotites that make up the lower portion of each unit. Many of the upper troctolitic parts of each unit are also associated with a strong layer-parallel mineral lamination,

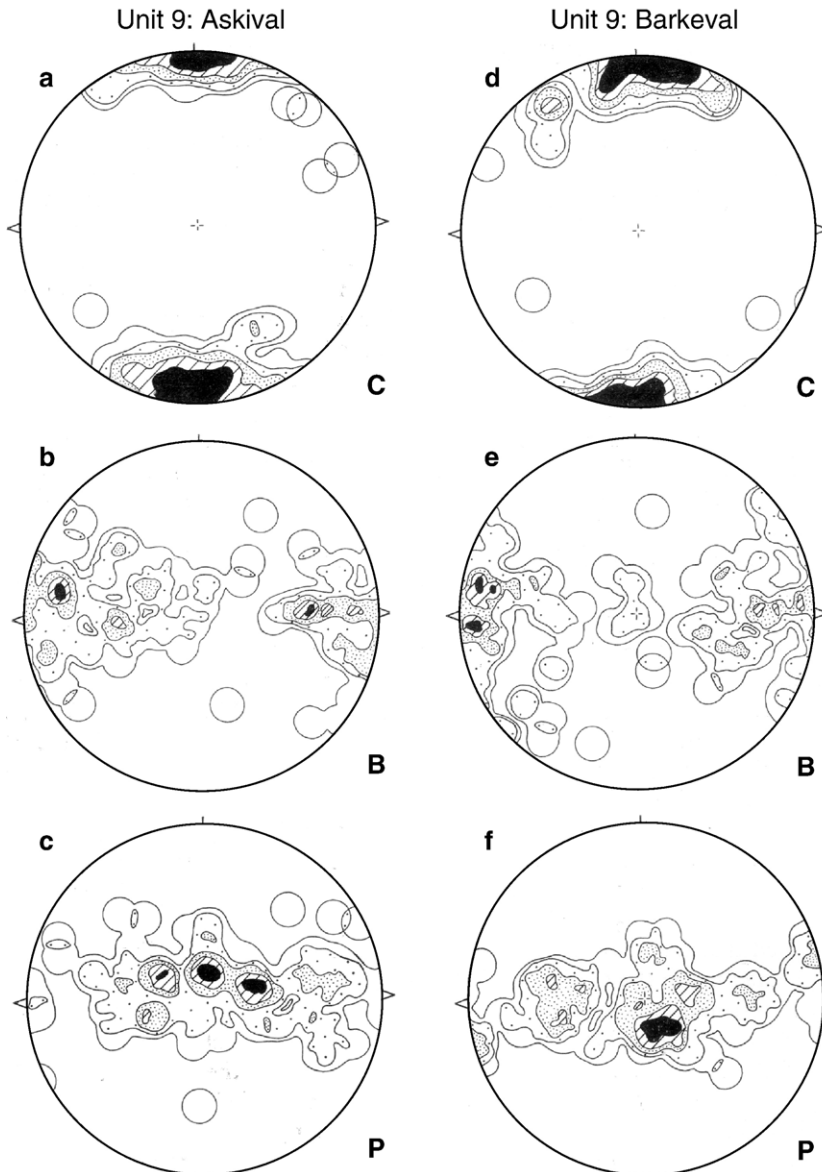


Fig. 4. A reproduction of Fig. 3 of Brothers (1964, p. 260), published with the permission of Oxford University Press (License No. 1642370664320). (a)–(c) C, B and P crystallographic directions (labeled) in 100 feldspar crystals from Unit 9 troctolite on the east face of Askival Plateau, Rum; contours at 1%, 2%, 4%, 6% and 8%, per 1% area. The trace of the igneous lamination is aligned east–west, as indicated by arrowheads on the primitive circle. (d)–(f) C, B and P crystallographic directions (labeled) in 100 feldspar crystals from Unit 9 troctolite below Barkeval, Rum; contours at 1%, 2%, 4%, 6% and 8%, per 1% area. Note that the C direction corresponds to the pole of the albite twin plane (010), the B direction lies in 010 and is the bisectrix of an angle in an albite twin plane, and the P direction is defined as the pole to the plane containing C and B. The B direction was inferred by Brothers to approximate the plagioclase *c*-axis direction.

Table 1

Anisotropy of magnetic susceptibility data for rocks of the Eastern Layered Series ( $K_{\text{mean}}$  presented in  $10^{-3}$  SI)

Site	Unit no.	$K_{\text{mean}}$	$K_1$	$K_3$	$P'$	$F$	$L$	$T$	Lithology
Sites 1–11									
1	10	3.75	0/340	87/072	1.13	1.09	1.04	0.358	Tr
2	9	5.88	3/308	54/212	1.08	1.04	1.04	−0.02	Tr
3	8	15.4	2/312	69/047	1.04	1.02	1.02	−0.01	Pe
4	11	0.63	1/131	76/043	1.05	1.04	1.01	0.592	Tr
5	10	1.5	5/155	84/031	1.06	1.05	1.01	0.658	Tr
6	10	2.82	12/296	67/052	1.08	1.04	1.04	−0.02	Tr
7	9	3.28	34/219	56/025	1.06	1.04	1.02	0.32	Tr
8	8	5.32	22/157	61/013	1.05	1.04	1.01	0.592	Tr
9	10	0.34	7/263	80/015	1.06	1.04	1.02	0.32	Pe
10	9	1.38	3/317	83/069	1.16	1.1	1.05	0.343	OG
11	9	6.09	6/317	81/088	1.43	1.32	1.05	0.704	Tr
Traverse A Unit 10									
1		0.68	3/158	47/057	1.04	1.03	1.01	0.493	Pe
2		2.64	31/174	50/029	1.03	1.02	1.01	0.327	Pe
3		1.4	16/167	65/032	1.06	1.05	1.01	0.658	Pe
4		2.58	14/170	70/029	1.06	1.04	1.02	0.32	Pe
5		2.38	14/173	74/036	1.04	1.03	1.01	0.493	Pe
6		1.87	29/254	56/023	1.03	1.02	1.01	0.327	Pe
7		2.91	14/168	72/031	1.09	1.07	1.01	0.741	Pe
8		2.91	6/309	77/052	1.06	1.05	1.01	0.658	Pe
9		2.06	8/295	79/068	1.04	1.03	1.01	0.493	Pe
10		0.95	6/320	62/075	1.03	1.02	1.01	0.327	Pe
11		1.6	15/163	66/039	1.05	1.04	1.01	0.592	Pe
12		2.84	43/216	46/054	1.04	1.03	1.01	0.493	Pe
13		2.96	42/324	53/286	1.03	1.01	1.02	−0.34	Pe
14		3.96	10/186	76/058	1.08	1.06	1.01	0.706	Pe
15		2.96	25/207	62/057	1.06	1.04	1.02	0.32	Pe
16		2.81	29/260	60/066	1.07	1.05	1.02	0.415	Pe
17		3.48	25/264	62/070	1.07	1.04	1.03	0.126	Pe
18		2.65	26/260	65/032	1.12	1.09	1.02	0.62	Pe
19		2.15	59/256	59/073	1.07	1.04	1.03	0.126	Pe
20		2.87	39/249	52/075	1.08	1.06	1.02	0.485	Pe
21		3.29	25/271	56/060	1.05	1.04	1.01	0.592	Pe
22		1.88	7/302	85/318	1.07	1.05	1.02	0.415	Pe
23		1.28	13/262	76/299	1.05	1.04	1.01	0.592	Pe
24		1.26	10/259	76/299	1.1	1.08	1.01	0.769	Pe
25		1.76	32/321	63/334	1.02	1.01	1.01	0	Tr
26		0.44	2/141	74/051	1.09	1.07	1.01	0.741	Tr
27		0.37	13/215	49/290	1.05	1.03	1.02	0.188	Tr
28		1.2	2/157	79/014	1.05	1.03	1.02	0.188	Tr
29		0.02	8/291	73/047	1.03	1	1.03	−1	Tr
30		0.02	2/314	73/037	1.05	1.04	1.01	0.592	Tr
31		1.04	15/344	62/046	1.5	1.39	1.04	0.789	Tr
32		0.01	4/298	84/068	1.06	1.04	1.02	0.32	Tr
33		1.04	1/256	73/358	1.04	1.02	1.02	−0.01	OG
34		0.37	2/312	67/048	1.1	1.08	1.01	0.769	OG
Traverse B Unit 10									
1		2.05	8/307	75/069	1.04	1.03	1.01	0.493	Pe
2		5.07	10/278	64/014	1.04	1.03	1.01	0.493	Pe
3		2.95	6/291	78/310	1.05	1.03	1.02	0.188	Pe
4		12.6	25/244	62/052	1.07	1.05	1.02	0.415	Pe
5		7.59	37/220	53/042	1.07	1.05	1.02	0.415	Pe
6		2.58	12/324	76/025	1.04	1.01	1.03	−0.51	Tr
7		4.45	34/288	40/303	1.03	1.02	1.01	0.327	Tr
8		2.06	4/284	70/027	1.06	1.04	1.02	0.32	Tr
9		1.94	6/295	64/037	1.05	1.04	1.01	0.592	Tr

(continued on next page)

Table 1 (continued)

Site	Unit no.	$K_{\text{mean}}$	$K_1$	$K_3$	$P'$	$F$	$L$	$T$	Lithology
Traverse B	Unit 10								
10		4.17	3/287	66/023	1.11	1.1	1	0.937	OG

Tr, Pe and OG represent the troctolite, peridotite and olivine gabbro lithologies, respectively.

generally defined by the planar arrangement of tabular plagioclase crystals. These plagioclases may exhibit compactional draping around olivine crystals or clinopyroxene oikocrysts (Fig. 3b) (Emeleus et al., 1996). Notably, large (1 cm) clinopyroxene oikocrysts in laminated troctolite may contain randomly oriented plagioclase grains, which tend to be smaller than those outside the oikocrysts (Holness et al., 2007). The peridotites are also locally laminated, in which case the fabric is carried by the preferred orientation of tabular olivine crystals. Small-scale layering throughout the Eastern Layered Series generally has the same orientation as the cyclic units that dip toward the centre of the intrusion, striking parallel to the outer contacts of the Eastern Layered Series, and dipping gently ( $<20^\circ$ ) toward a central section of the Long Loch Fault (Fig. 1) (Emeleus et al., 1996).

Although some layers are modally graded, grain size variation in the Eastern Layered Series is uncommon. Syn-magmatic (soft-sediment) deformation features, however, such as slump folds, load and flame structures, and syn-sedimentary faulting (Fig. 3c and d) are frequently observed in the Eastern Layered Series (Emeleus et al., 1996). These structures are best observed in the upper parts of the cyclic units where peridotite and troctolite are intimately interlayered with each other, e.g. in Units 7, 11 and 12, though Units 9 and 10 are notably deficient in such structures. In most cases, deformation of layering seems to have occurred as poorly consolidated crystal mush collapsed and slumped down on surfaces too steep to support it, developing structures that generally give a downdip sense of movement. Emeleus et al. (1996) also note that thick troctolite layers show the most evidence for simultaneous slumping, loading and shearing, so that 'the upper portion of the loaded layer is a smeared-out mixture of mafic laminae, recumbent fold limbs and heterogeneous allivalite.' This deformation becomes more intense toward the Long Loch Fault, with where massive slump sheets and mélanges deform sequences of layering.

Infrequent alignments of minerals on layer and lamination planes (magmatic lineations) have been reported from field and thin-section studies of Units 8, 9 and 10 (e.g. Brothers, 1964; Housden et al., 1996). In particular, Housden et al. (1996) noted the presence of a weak lineation of elongate plagioclase and sub-equant olivine grains in the troctolite of Unit 10 in the field,

oriented parallel to the strike of layering and lamination planes, an observation that is corroborated by fieldwork on Unit 10 in this study. Several peridotite sites studied in Unit 10 by Housden et al. (1996) display a clearly visible lineation of tabular olivine grains, also parallel to strike of lamination surfaces (e.g. Site 7, P101, Housden et al., 1996). Brothers (1964) carried out a detailed petrofabric analysis of feldspar orientation in the troctolites of Units 8, 9, and 10. His Universal Stage study on field-oriented thin-sections mapped out the presence of weak linear arrangements of feldspar crystallographic  $c$ -axes (crystallographic preferred orientation; CPO) that consistently trend approximately parallel to the strike of the pervasive mineral lamination (Fig. 4). Though Brothers (1964) mapped out consistent plagioclase CPO fabrics from the troctolites of Units 8, 9 and 10, his method was not sufficiently sensitive to distinguish a lineation defined by cumulus olivine in the troctolites or the peridotites of these cyclic units. However, he did demonstrate that the vast majority of olivine crystals in the peridotites and troctolites are aligned with their (010) faces parallel to the mineral lamination. Brothers (1964) was also careful to point out that his fabric measurements reflected orientation of a CPO only, and not a shape-preferred orientation (SPO), as the morphological habits of many of the original seed crystals may have been masked by subsequent intercumulus overgrowth.

Our thin-section observations on troctolites from Units 8, 9 and 10 reveal that plagioclase in the Eastern Layered Series troctolite shows little or no evidence for solid-state (crystal–plastic) deformation processes that might cause deviation of the SPO from the CPO. Dislocation of twin planes, mechanical twinning or recrystallisation microstructures are all absent from plagioclase grains carrying the mineral lamination. These observations are supported by the results of Tepley and Davidson (2003) that indicate primary magmatic zoning in plagioclase in the Eastern Layered Series troctolites, i.e. significant recrystallisation has not occurred. Lo Ré et al. (2003) also emphasize the coincident nature of the CPO and SPO in Unit 9, and Holness (2005) used quantitative textural measurements to argue that equilibration of textures was not widespread in the Eastern Layered Series, but instead operated locally, e.g. in the vicinity of the Unit 9 peridotite.

#### 4. Anisotropy of magnetic susceptibility analysis

##### 4.1. Introduction

The anisotropy of magnetic susceptibility (AMS) of a rock is controlled by the orientation (and to a certain extent the distribution) of ferromagnetic minerals (e.g.

magnetite) and to a lesser extent by the orientation of paramagnetic minerals (ferromagnesian phases) (Tarling and Hrouda, 1993). The maximum, intermediate, and minimum strength directions allow for the definition of a susceptibility ellipsoid with three principal susceptibility axes ( $K_1 \geq K_2 \geq K_3$ ). AMS fabric data are given by the orientation of  $K_1$  (the magnetic lineation) and of the

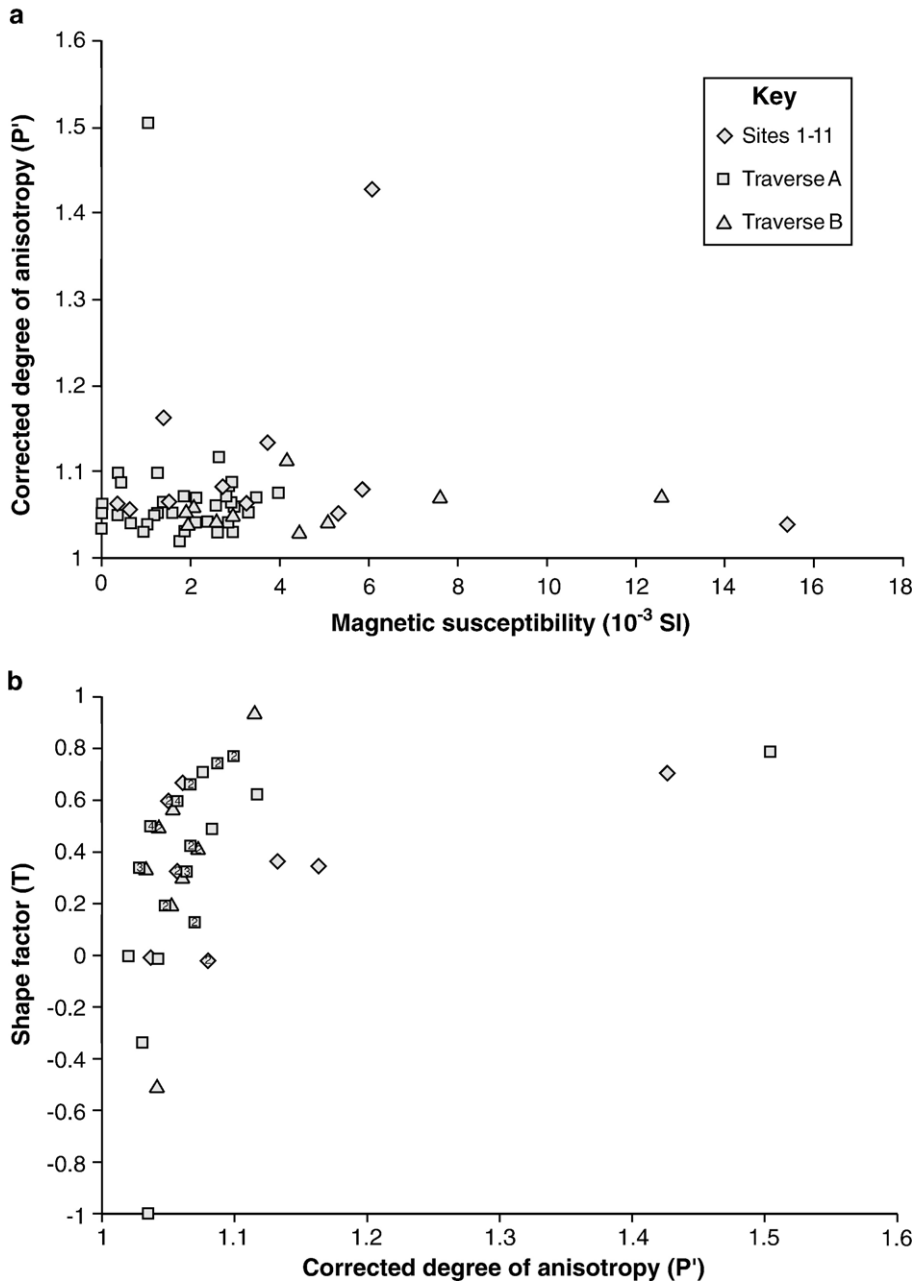


Fig. 5. (a) Plot of corrected degree of anisotropy  $P'$  vs. mean magnetic susceptibility  $K_{\text{mean}}$ , and (b) shape factor  $T$  vs. corrected degree of anisotropy  $P'$ , for all AMS data (see text for Discussion). For both plots, the diamond symbols represent Sites 1–11, the squares Traverse A and the triangles Traverse B. Numbers on symbols in (b) represent the number of samples that plot at an identical point on the graph.

plane ( $K_1$ ,  $K_2$ ) perpendicular to  $K_3$  (the magnetic foliation). The principal susceptibilities are also used to derive alternative combinations of magnitude parameters such as the bulk susceptibility,  $K_{\text{mean}} = (K_1 + K_2 + K_3)/3$ , the degree of magnetic lineation ( $L = K_1/K_2$ ) and the degree of magnetic foliation ( $F = K_2/K_3$ ). The degree of anisotropy is given by  $P = K_1/K_3$ , however, a corrected degree of anisotropy that accounts for the intermediate axis ( $P' = \exp\sqrt{2[(\eta_1 - \eta)^2 + (\eta_2 - \eta)^2 + (\eta_3 - \eta)^2]}$ , where  $\eta = (\eta_1 + \eta_2 + \eta_3)/3$ ,  $\eta_1 = \ln K_1$ ,  $\eta_2 = \ln K_2$ ,  $\eta_3 = \ln K_3$ ) is usually taken as a measure of the strength of the magnetic fabric (Jelinek, 1981); a value of  $P' = 1$  describes a perfectly isotropic fabric, a  $P'$  value of 1.15 describes a sample with 15% anisotropy, and so on. The shape parameter ( $T = [2\ln(K_2/K_3)/(\ln(K_1/K_3)) - 1]$ ) is a quantitative measure of the shape of the susceptibility ellipsoid, ranging from +1 where purely foliated (oblate) to -1 where purely lineated (prolate).

#### 4.2. Sampling procedure

Block samples were collected at 11 sites from Units 8, 9, 10 and Unit 11 of the Eastern Layered Series, in a relatively small area extending across the northern slopes of Hallival and Barkeval (Fig. 1; Table 1). Samples were generally taken from the troctolites of each unit, so that AMS data could be compared with measurements carried out on small-scale structures that are much more common in the troctolite portions of units. None of the samples were collected from harrisite, a coarse-grained feldspathic peridotite characterised by skeletal olivine crystals that frequently display preferential orientation perpendicular to the plane of layering (comb layering). Oriented blocks were collected in the field away from faults and fractures and were precisely positioned to within 10 m using GPS. AMS measurements were carried out at Princeton University (USA) using a Sapphire Instruments SI2 low-field susceptibility apparatus. Site means were calculated from measurements on an average of 6 specimens drilled from each block sample, following the method outlined by Jelinek (1978).

In addition, the magnetic fabrics were analysed of existing sample sets from two detailed traverses that were both carried out through the peridotite and troctolite sections of Unit 10 (the type unit of the Eastern Layered Series) on the north side of Hallival (Fig. 1d), so that the importance of within-unit fabric variation could be assessed. One of these, Traverse A, comprises 34 sites through Unit 10 and is approximately 150 m long. Traverse A was sampled by Housden et al. (1996), who presented a detailed study of the magnetic susceptibilities and magnetic rock properties of Unit

10. Traverse B consists of 10 sites, is approximately 130 m long and is located about 150 m east of Traverse A (Fig. 1d). Traverse B was originally sampled as part of a palaeomagnetic study carried out on Rum by Dagley and Musset (1981). Samples for both traverses were collected as oriented and closely spaced drilled cores; 458 specimens from Traverse A (approximately 6 per site), and 35 specimens from Traverse B (approximately 3 per site). Neither of the two studies above analysed

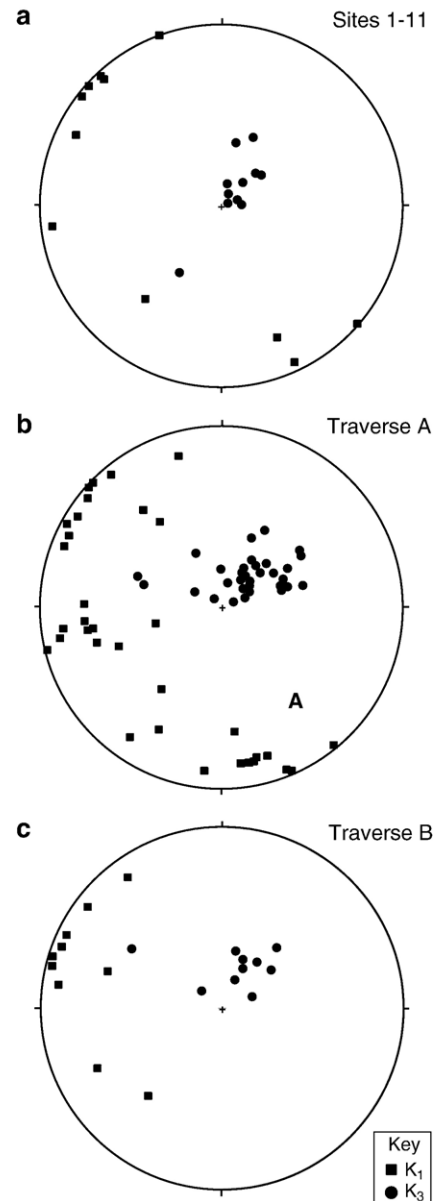


Fig. 6. Equal-area lower hemisphere plots for Anisotropy of Magnetic Susceptibility data. (a)–(c) Poles to magnetic foliation planes (circles) and magnetic lineations (squares) for Sites 1–11, Traverse A, and Traverse B, respectively.

samples from Traverses A and B for AMS fabrics. The samples from Traverses A and B were also analysed on a Sapphire Instruments SI2 low-field susceptibility apparatus at Princeton University, and site means were again calculated from drill cores after Jelinek (1978).

4.3. AMS results

4.3.1. Magnetic susceptibility

Magnetic susceptibility data for all samples of the Eastern Layered Series rocks are given in Table 1, together with the other principal magnetic features measured.  $K_{mean}$  values of individual stations throughout the Eastern Layered Series range between 0.01 and  $15.4 \times 10^{-3}$  SI.  $K_{mean}$  appears to exhibit a general decrease with stratigraphic height (Unit 8:  $5.32\text{--}15.4 \times 10^{-3}$  SI, Unit 9:  $1.38\text{--}6.09 \times 10^{-3}$  SI, Unit 10:  $1.5\text{--}3.75 \times 10^{-3}$  SI and Unit 11:  $0.63 \times 10^{-3}$  SI). Both of the traverses of Unit 10 in the north of the Eastern

Layered Series have comparatively low susceptibilities: Traverse A:  $0.01\text{--}3.96 \times 10^{-3}$  SI, and Traverse B:  $1.94\text{--}12.6 \times 10^{-3}$  SI. The more detailed Traverse A shows a general decrease in  $K_{mean}$  with stratigraphic height through Unit 10, a feature that is not as well reflected in Traverse B.

4.3.2. AMS fabrics

$P'$  measured for the Eastern Layered Series sample set (excluding Traverses A and B) varies between 1.04 and 1.43, and averages at 1.11 (Table 1). It is therefore generally of moderate strength, between 1.05 and 1.15 for 80% of samples. Values for  $P'$  for Traverses A and B are similar to those quoted above, varying between 1.02 and 1.5 (average: 1.07) and 1.04 and 1.11 (average: 1.06), respectively. Lateral or stratigraphic variation in  $P'$ , or correlation of  $P'$  with  $K_{mean}$ , throughout the Eastern Layered Series is absent (Fig. 5A). Values of  $T$  range between  $-0.02$  and 0.704 for Sites 1–11, with an

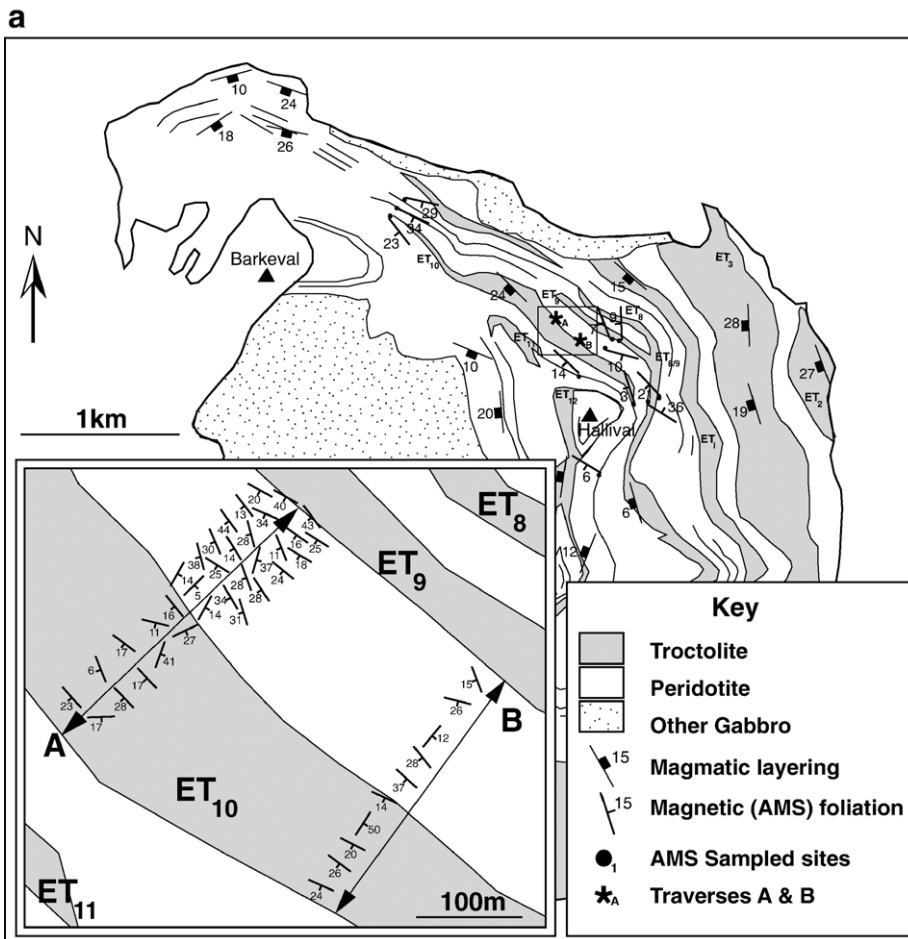


Fig. 7. (a) Magnetic foliation data and (b) magnetic lineation data, for the Eastern Layered Series. Traverses A and B are both taken along the line of section illustrated. In the case of the peridotite portion of Traverse A, only the approximate positions of sampled sites are shown.

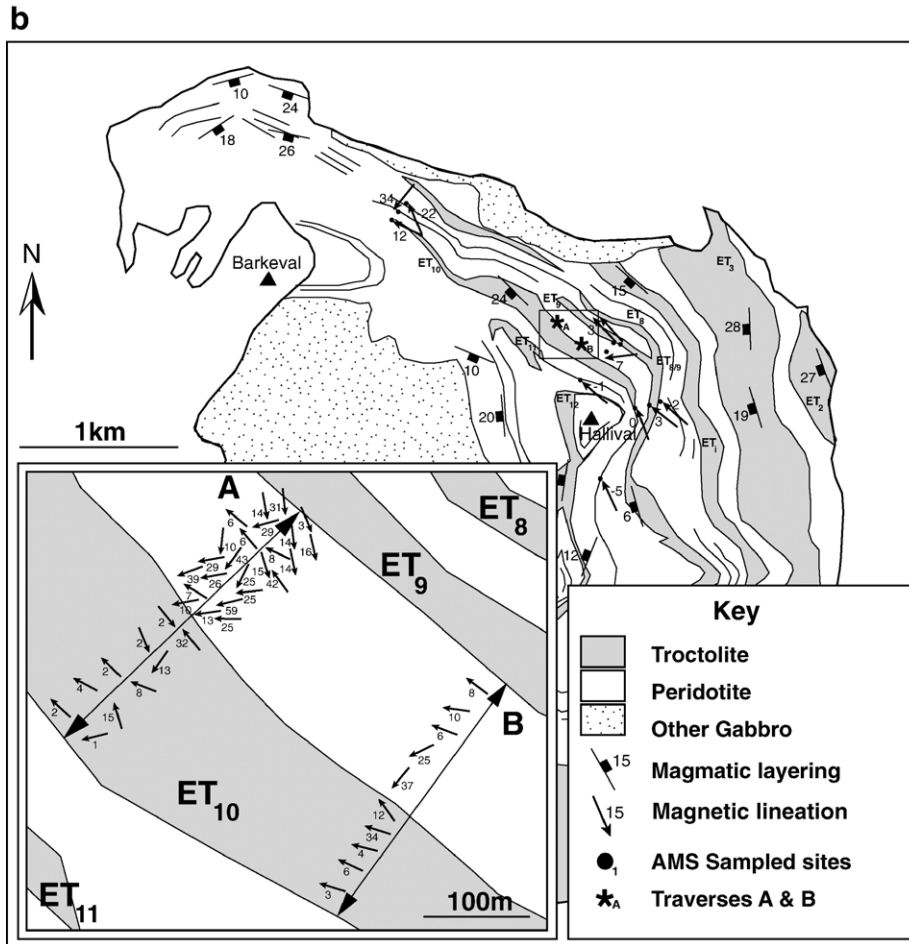


Fig. 7 (continued).

average value of 0.349. Traverses A and B reveal  $T$ -values of  $-1$  to 0.769 (average: 0.369) and  $-0.51$  to 0.937 (average: 0.367), respectively. The shape of the magnetic fabric ellipsoid is therefore oblate–triaxial (Fig. 5B).

The orientations of the AMS fabrics from Sites 1 to 11 and Traverses A and B are characterised by one dominant trend throughout the study area. Magnetic foliations chiefly strike NW–SE and mostly dip quite shallowly to the SW, parallel to visible layering and mineral laminations (Figs. 6 and 7A). Magnetic lineations associated with this trend often exhibit a NW–SE trend with shallow plunges (Figs. 6 and 7B). A second and subordinate (SW) trend of the magnetic lineation is observed towards the middle of Unit 10 in both traverses close to the peridotite–troctolite boundary. Here, the magnetic foliation may remain oriented parallel to layering, so that the magnetic lineations trend nearly downdip rather than parallel to the strike of magnetic

foliation planes (Figs. 6 and 7). In a small number of samples (e.g. in Traverses A and B), NW–SE trending magnetic lineations are associated with magnetic foliations that strike NE–SW and dip SE (see Figs. 6 and 7).

## 5. Discussion

### 5.1. Magnetic susceptibility of the Eastern Layered Series

The bulk magnetic susceptibility of a rock depends on the intrinsic magnetic susceptibilities and proportions of the rock-forming minerals (Borradaile and Jackson, 2004). Magnetic susceptibility values of Eastern Layered Series rocks measured in this study are mostly close to  $10^{-3}$  SI (usually considered as reflecting ferromagnetic behavior in rocks; Rochette, 1987). Housden et al. (1996) carried out magnetic hysteresis

studies on all of the samples from Traverse A of this study, measuring the high-field paramagnetic susceptibility of the peridotites and troctolites. They were able to show that the paramagnetic contribution (with a range of  $0.1\text{--}0.4 \times 10^{-3}$  SI, average:  $0.24 \times 10^{-3}$  SI, for 20 representative samples through Traverse A) corresponds to the variation in olivine/plagioclase ratio, or rock density, throughout Unit 10, implying that olivine was the dominant paramagnetic mineral in Traverse A. By subsequently separating the paramagnetic and ferromagnetic fractions, Housden et al. (1996) showed that the total and the ferromagnetic contributions exhibit the same susceptibility trends, suggesting that the magnetic susceptibility is dominated by a ferromagnetic phase. However, they also noted that in several troctolite samples, the paramagnetic fraction dominated the susceptibility over the ferromagnetic fraction, where the amount of ferromagnetic carrier was  $<0.1\%$  by weight of olivine. Thermomagnetic analyses carried out by Housden et al. (1996) on samples from Traverse A revealed one Curie temperature characteristic of all samples;  $575 \pm 5$  °C, suggestive of the presence of nearly pure magnetite. A calculated Curie temperature of  $25 \pm 50$  °C for chromite allowed Housden et al. (1996) to estimate that this mineral had a negligible contribution to the magnetic susceptibility of Unit 10.

Our magnetic susceptibility data support Housden et al. (1996), that magnetite, for the most part, dominates the susceptibility of Eastern Layered Series units. This is particularly true of the peridotite samples measured in each of Traverses A and B, where the high olivine content has resulted in a corresponding high magnetite content (see above and Putnis, 1979; Moseley, 1984; Housden et al., 1996). However, several of our samples (e.g. Traverse A troctolite; see Table 1) have magnetic susceptibilities less than  $0.24 \times 10^{-3}$  SI, the average quoted by Housden et al. (1996) for paramagnetic behaviour, and these may instead reflect a contribution by olivine, the dominant paramagnetic mineral.

### 5.2. Relationship between AMS and olivine orientation

The occurrence of magnetite as crystallographically constrained platelets in olivine in the Eastern Layered Series troctolites was first noted by Judd (1885). Subsequent work by Putnis (1979), Moseley (1984) and Housden et al. (1996) shed further light on their origin and mode of occurrence on Rum, as described above. However, although ferromagnetic inclusions are a common feature in certain minerals, they may complicate the interpretation of a rock magnetic fabric (cf. Rochette et al., 1992).

Lagroix and Borradaile (2000) carried out a study of the relationship between low-field AMS and crystalline structure for several different mineral phases and noted the effects of ferromagnetic inclusions on the paramagnetic behaviour of each phase. Though olivine was not one of the minerals studied, orthopyroxene, which shares the same (orthorhombic) crystallographic symmetry was included. Lagroix and Borradaile (2000) found that orthopyroxene, with numerous amounts of small opaque inclusions ( $0.01\text{--}0.62$  vol.% of the orthopyroxene), exhibited parallelism of  $K_1$  with the maximum crystallographic  $c$ -axis. However, both of the other two principal susceptibility axes lie at angles to the other two crystallographic axes, so that the AMS foliation plane could not be correlated with a simple crystallographic plane. Lagroix and Borradaile (2000) deduced that ferromagnetic inclusions were oriented obliquely to the crystal lattice symmetry elements. Despite the high crystal symmetry of orthopyroxene, the inclusions completely masked the AMS expected from the intrinsic symmetry of anisotropy of the orthopyroxene crystals. Lagroix and Borradaile (2000) also noted that as  $K_{\text{mean}}/K_{\text{para}}$  (where  $K_{\text{para}}$  is the paramagnetic susceptibility), tends towards 1, the less likely it is that there are ferromagnetic inclusions present, and that expected crystallographic/susceptibility axes relationships will be observed. This was corroborated by Ferré et al. (2005), who measured the high-field AMS of a gem grade olivine sample, and found that its principal paramagnetic susceptibility axes had the following relationship to the olivine crystallographic axes:  $K_{\text{para1}} = [001]_{\text{olivine}}$ ,  $K_{\text{para2}} = [100]_{\text{olivine}}$  and  $K_{\text{para3}} = [010]_{\text{olivine}}$ .

As described above, AMS fabrics from the top of the troctolites of Units 8, 9, and 10 reveal one dominant trend throughout the northern part of the Eastern Layered Series, despite the recorded presence of magnetite inclusions in olivine grains, though minor, within-unit, variation occurs in Unit 10 (Traverses A and B) and is discussed below. Magnetic foliations generally strike NW–SE and dip shallowly to the SW, and magnetic lineations show a broadly NW–SE trend with extremely gentle plunges. The magnetic foliations are thus typically parallel to the macroscopic magmatic layering at both the cyclic unit scale and at smaller (mineral lamination) scales. Magnetic lineations typically trend sub-parallel to the strike of these planes, and may plunge in either direction. Although AMS ellipsoid shapes in the Eastern Layered Series are mainly triaxial to strongly oblate, the consistency of the magnetic lineations within the dominant fabric group throughout Units 8, 9, and 10 indicate that they may also (in addition to the

magnetic foliations) be interpreted as valid linear structural elements.

The magnetic susceptibility data summarised above, together with the detailed rock magnetic experiments, thermomagnetic analyses and petrological observations of Housden et al. (1996) suggest that the magnetic susceptibility is predominantly carried by magnetite, and secondarily by olivine. We argue that the AMS represents normal fabrics controlled by the shape-preferred orientation of magnetite grains and to a much lesser extent by the crystallographic orientation of olivine. We thus suggest that the dominant magnetic fabric trend reflects a primary silicate fabric carried by both magnetite and olivine. It is therefore proposed that the magnetite platelets must be oriented such that they do not obscure, but rather enhance, the olivine fabric, i.e. that the magnetic fabric has  $K_1 = [001]_{\text{olivine}}$ ,  $K_2 = [100]_{\text{olivine}}$  and  $K_3 = [010]_{\text{olivine}}$ . These propositions are supported by the following lines of evidence:

1. Observations by both Moseley (1984) and Housden et al. (1996) that the magnetite platelets in Unit 10 olivines display a strong preferred orientation relationship parallel to the olivine crystallographic  $c$ -axis (see Section 3.1).
2. The orientation of the magnetic foliation plane in the dominant magnetic fabric group matches that of the magmatic layering (at all scales) and of the mineral lamination. Furthermore, Brothers' (1964) Universal Stage measurements showed that tabular olivine grains in peridotite are oriented with their (010) faces parallel to layering.
3. The magnetic lineation in the dominant magnetic fabric group has a similar orientation to crystallographic preferred orientations of plagioclase on mineral lamination planes in troctolite (cf. Brothers, 1964), and also to visible plagioclase lineations in troctolite in Units 9 and 10, suggesting that the magnetic fabric observed may reflect an existing silicate fabric.
4. Some samples in Traverse A exhibit susceptibilities below that of the average  $K_{\text{para}}$  estimated by Housden et al. (1996). The magnetic fabric of these rocks is therefore believed to be controlled by olivine alone, with minimal influence from magnetite inclusions. Nonetheless, the magnetic fabric orientation of these sites typically conforms to the dominant trend described above.

The possibility of inverse fabrics (*sensu* Rochette et al., 1992) in the dominant magnetic fabric group is deemed unlikely based on the typical size of the magnetite platelets (see Section 3.1 and Housden

et al., 1996) and also on the fact that magnetic foliations in this group are parallel to mineral lamination and magmatic layering, as described above. However, as noted in Section 4.3.2 a small group of samples in Traverses A and B (e.g. see Fig. 5A and B) exhibit magnetic lineations that are similar to those in the dominant fabric group, yet have magnetic foliations that are perpendicular to the mineral lamination/magmatic layering. These may represent intermediate fabrics (*sensu* Rochette et al., 1992; Ferré et al., 2002) and are viewed here with caution. Several samples have magnetic fabrics whose foliations parallel layering, yet have lineations oriented down-dip on foliation planes. These samples are discussed in more detail in the next section.

### 5.3. Magmatic lineations in the Eastern Layered Series?

Emeleus et al. (1996) suggested that the common occurrence of soft-sediment deformation structures in the Rum cumulates indicates a significant degree of reworking following floor accumulation of crystals. Indeed, they note that roof cumulates are absent in the few localities where the former magma chamber roof is exposed. However, they also state that the mechanism through which crystals were transported to the floor remains unclear, and may have involved simple crystal settling or roof-derived crystal-laden plumes. Recent studies by Worrell (2002) and Tepley and Davidson (2003) have also invoked current activity as a mechanism for accumulating crystals from the roof and the interior of the magma chamber to the floor.

Planar fabrics (without an associated lineation) such as mineral laminations in cumulates have been ascribed to processes ranging from primary deposition of crystals from density currents and plumes to compaction-related solid-state recrystallisation (see Irvine, 1980; Irvine et al., 1998 for review). For example, Brothers (1964) suggested that his measurements on olivine crystals in the peridotite that indicated a preference for olivine to be oriented with (010) faces parallel to layering was representative of crystal settling processes. Consistent lineation data in rocks exhibiting magmatic layering are commonly taken as reliable evidence for magmatic flow within the plane of layering or lamination. Our field observations and magnetic fabric data both provide evidence for the occasional presence of a weak linear arrangement of crystals on mineral lamination/magnetic foliation planes. These linear fabrics might thus be interpreted as representing primary flow during magma emplacement into the Rum magma chamber, or as flow due to initial accumulation of crystals through plumes and density currents. Indeed, Brothers (1964) interpreted the

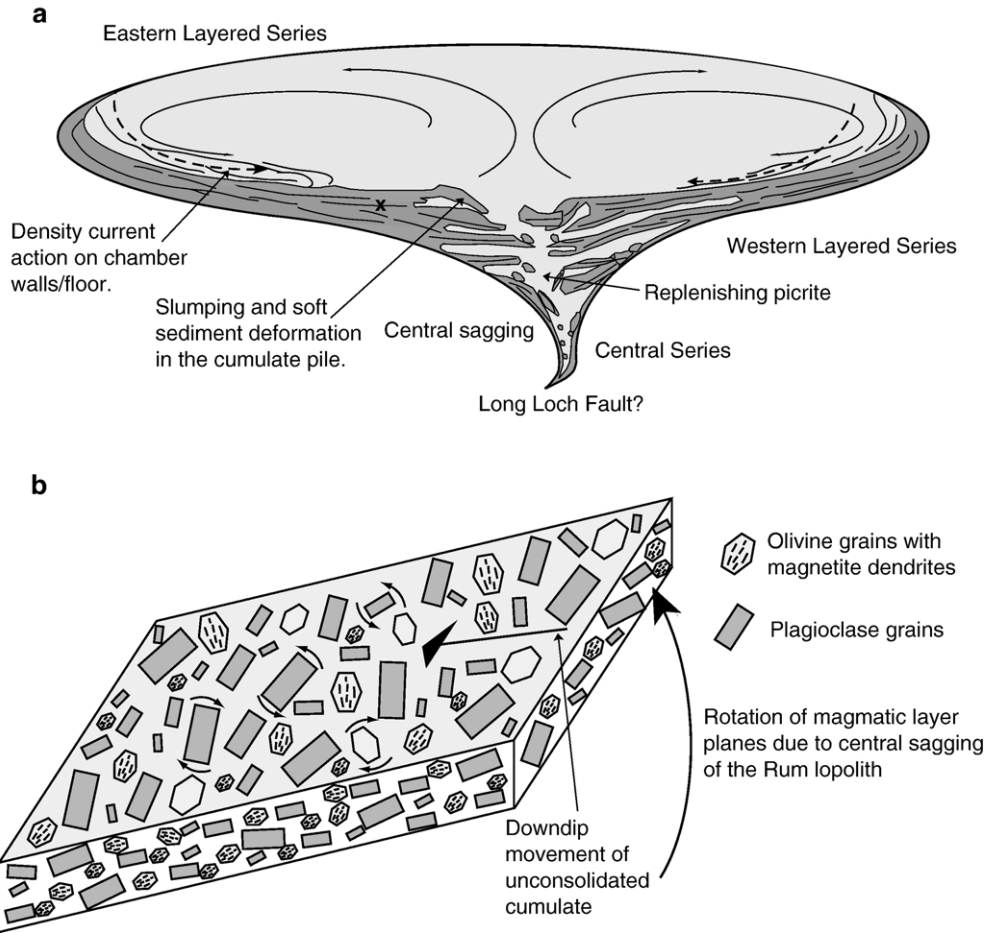


Fig. 8. (a) Schematic diagram of the Rum intrusion illustrating the proposed magma chamber processes leading to slumping and soft-sediment deformation of layering toward a central point along the Long Loch Fault. The point labelled X in the top part of the cumulate pile is where the processes illustrated in (b) are envisaged to occur. (b) Schematic sketch of a troctolite layer in the crystallising Rum cumulate pile (components of the figure are not to scale). Movement downdip of the crystal mush is associated with rotation inward of magmatic layer planes. This results in soft sediment deformation and weak lineations on layer planes oriented transverse to the direction of movement (arrows are drawn to indicate how crystals may become aligned). Note the formation of a mineral lamination in the plane of layering, possibly due in part to compaction-related processes (see text for discussion).

observed feldspar fabric data in the Eastern Layered Series as reflecting deposition from laminar flow in magma currents. He also noted that positioning of elongate particle axes transverse to current direction is an expected result of particles in suspension in laminar flow (Brothers, 1964, and references therein). Elongate clasts that are oriented perpendicular to current direction are also well documented in sedimentary rocks (e.g. Rust, 1972; Davies and Walker, 1974).

This study cannot unequivocally discount the notion of previous workers that observed lineations in the Rum Eastern Layered Series result from current activity, but proposes that another solution should also be considered. This solution is based primarily on the importance of field evidence in deformed cumulates and the confocal orientation of layering throughout the Eastern

Layered Series, and indeed the whole of the Rum Layered Suite, for late-stage central sagging of the intrusion toward the Long Loch Fault. The significance of such central sagging of layered units has been reported for a number of intrusions, e.g. the Skaergaard intrusion (McBirney and Nicolas, 1997), the Bushveld Complex (Carr et al., 1994) and the Rogaland Igneous Complex (Bolle et al., 2002).

Emeleus et al. (1996) postulate that compaction of the Rum cumulates is likely to have been a continuous process, and therefore significant thicknesses (>5 m) of unconsolidated cumulate would have only rarely been able to form. Assuming that central sagging was coincident with compaction-related processes, the upper several metres of cumulate directly below the magma–crystal mush interface could have been in

periodic movement, occasionally building up to unstable thicknesses and slumping to produce the dramatic soft-sediment deformation structures observed. We propose that periodic central sagging caused a reshuffling and sliding of grains over each other within the top several metres of the cumulate pile after accumulation of the crystals occurred (Fig. 8a and b). Olivine and plagioclase seed crystals were rotated within the plane of layering to give a subtle lineation oriented across the downdip direction of slumping/movement. The general lack of crystal plastic strain (e.g. deformation twinning in plagioclase) suggests that this slumping occurred whilst the Rum cumulate pile still contained a significant melt fraction (see Section 3.2). The topmost part of the crystal pile, under the influence of gravity, was therefore able to behave viscously (cf. Nicolas, 1992). Magnetic fabrics that exhibit lineations oriented downdip on foliation planes might represent fabrics caused by more abrupt slumping of crystal mush in a downdip direction transported over a larger distance. Interestingly, the study of Brothers (1964) also included grain orientation measurements on a layered trough structure from the Skaergaard intrusion, in which he describes preferred linear alignments of crystals that are oriented parallel to magma current orientation. The fast density current flows invoked by Wager and Brown (1968) to produce this concave trough structure studied by Brothers (1964) may be analogous to high-energy thixotropic flows in viscous unconsolidated crystal mushes as they slumped downdip, locally producing lineations that also plunged downdip on layer planes.

We consider that the model presented above, in which weak magmatic lineations in the Rum cumulates were produced during soft-sediment deformation as a result of central sagging, offers a mechanism by which this essentially postcumulus process could overprint any primary flow fabrics present. The petrographic observation of Holness et al. (2007) that laminated troctolite contains clinopyroxene oikocrysts, which in turn contain small randomly oriented plagioclase grains, supports the notion that postcumulus overgrowth and reorientation of grains in the cumulate pile may have occurred.

## 6. Summary

We have combined field evidence and AMS fabric data that indicate the presence of weak linear fabrics in cumulates of Units 8, 9 and 10 of the Rum Eastern Layered Series. The dominant fabric group in the AMS dataset exhibits magnetic foliations oriented NW–SE, parallel to magmatic layering and mineral lamination, and dipping shallowly to the SW, together with a

magnetic lineation that trends approximately NW or SE, parallel to strike of the magnetic foliation planes, and plunging very shallowly in either direction. A subordinate group in which magnetic lineations plunge downdip on magnetic foliation planes (the latter remain oriented similar to the above trend) is also observed. Two detailed AMS traverses carried out through Unit 10 north of Hallival confirm the consistency of the magnetic fabric measurements. Magnetic susceptibility data presented here confirm the observations from rock magnetic experiments of previous studies that magnetite dominates the susceptibility, with a secondary control by olivine. We believe that the consistency between the field observations and the magnetic fabric dataset warrants the conclusion that magnetite platelets in olivine crystals reflect the olivine crystallographic preferred orientation.

Despite widespread evidence for central subsidence of the Rum Layered Suite, previous studies have placed little emphasis on quantifying the effects of this subsidence on the textures of partially consolidated Rum cumulates. A model is proposed here which suggests that weak lineations observed in the field and in the AMS dataset developed in the top several metres of the cumulate pile, following crystal accumulation and synchronous with central sagging and deformation of the crystal mush.

## Acknowledgements

We acknowledge and thank J. Housden and P. Dagley for providing core material for AMS measurements from earlier palaeomagnetic studies on Unit 10. Scottish Natural Heritage is thanked for permission to carry out fieldwork on Rum. Mike Petronis and Carl Stevenson are thanked for constructive criticism and discussion. The positive and insightful comments provided by two anonymous reviewers are gratefully acknowledged. B.O'D. acknowledges receipt of an Irish Research Council for Science Engineering and Technology (IRCSET) grant for post-graduate study at Trinity College Dublin, and V.R.T. acknowledges a Science Foundation Ireland (SFI) research grant.

## References

- Bédard, J.H., Sparks, R.S.J., Renner, R., Cheadle, M.J., Hallworth, M.A., 1988. Peridotite sills and metasomatic gabbros in the Eastern Layered Series of the Rhum complex. *Journal of the Geological Society* 145, 207–224.
- Bolle, O., Diot, H., Duchesne, J.C., 2000. Magnetic fabric and deformation in charnockitic igneous rocks of the Bjerkreim–Sokndal layered intrusion (Rogaland, Southwest Norway). *Journal of Structural Geology* 22, 647–667.

- Bolle, O., Trindade, R.I.F., Bouchez, J.L., Duchesne, J.C., 2002. Imaging downward granitic magma transport in the Rogaland Igneous Complex, SW Norway. *Terra Nova* 14, 87–92.
- Borradaile, G.J., Jackson, M., 2004. Anisotropy of magnetic susceptibility (AMS): magnetic petrofabrics of deformed rocks. In: Martin Hernandez, F., Lünenburg, C.M., Aubourg, C., Jackson, M. (Eds.), *Magnetic Fabric: Methods and Applications*. Geological Society of London, Special Publication, vol. 238, pp. 299–360.
- Bouchez, J.L., 1997. Granite is never isotropic: an introduction to AMS studies of granitic rocks. In: Bouchez, J.L., Hutton, D.H.W., Stephens, W.E. (Eds.), *Granite: From Segregation of Melt to Emplacement Fabrics*. Kluwer Academic Publishers, Dordrecht, pp. 95–112.
- Brothers, R.N., 1964. Petrofabric analysis of Rhum and Skaergaard Layered Rocks. *Journal of Petrology* 5, 255–274.
- Brown, G.M., 1956. The layered ultrabasic rocks of Rhum, Inner Hebrides. *Philosophical Transactions of the Royal Society. B* 240, 1–53.
- Butcher, A.R., Young, I.M., Faithfull, J.W., 1985. Finger structures in the Rhum Complex. *Geological Magazine* 122, 503–518.
- Butcher, A.R., Pirrie, D., Prichard, H.M., Fisher, P., 1999. Platinum-group mineralization in the Rhum layered intrusion, Scottish Hebrides, UK. *Journal of the Geological Society, London* 156, 213–216.
- Carr, H.W., Groves, D.I., Cawthorne, R.G., 1994. The importance of synmagmatic deformation in the formation of Merensky Reef pot-holes in the Bushveld Complex. *Economic Geology* 89, 1398–1410.
- Dagley, P., Musset, A.E., 1981. Palaeomagnetism of the British Tertiary Igneous Province: Rhum and Canna. *Journal of the Royal Astronomical Society* 65, 475–491.
- Davies, I.C., Walker, R.G., 1974. Transport and deposition of resedimented conglomerates: The Cap Enrage Formation, Cambro-Ordovician, Gaspé, Quebec. *Journal of Sedimentary Petrology* 44, 1200–1216.
- Dunham, A.C., Wadsworth, W.J., 1978. Cryptic variation in the Rhum layered intrusion. *Mineralogical Magazine* 42, 347–356.
- Emeleus, C.H., 1987. The Rhum Layered Complex, Inner Hebrides, Scotland. In: Parsons, I. (Ed.), *Origins of Igneous Layering*. D. Reidel Publishing Company, pp. 263–286.
- Emeleus, C.H., Bell, B.R., 2005. *British Regional Geology: The Palaeogene Volcanic Districts of Scotland*, Fourth edition. British Geological Survey, Nottingham.
- Emeleus, C.H., Cheadle, M.J., Hunter, R.H., Upton, B.G.J., Wadsworth, W.J., 1996. The Rhum Layered Suite. In: Cawthorne, R.G. (Ed.), *Layered Igneous Rocks*. Elsevier, Amsterdam, pp. 403–440.
- Ferré, E.C., Bordarier, C., Marsh, J.S., 2002. Magma flow inferred from AMS fabrics in a layered mafic sill, Insizwa, South Africa. *Tectonophysics* 354, 1–23.
- Ferré, E.C., Tikoff, B., Jackson, M., 2005. The magnetic anisotropy of mantle peridotites: example from the Twin Sisters dunite, Washington. *Tectonophysics* 398, 141–166.
- Hargraves, R.B., Chan, C.Y., Johnson, D., 1991. Distribution anisotropy: the cause of AMS in igneous rocks? *Geophysical Research Letters* 18, 2193–2196.
- Holness, M.B., 2005. Spatial constraints on magma chamber replenishment events from textural observations of cumulates: the Rhum Layered Intrusion, Scotland. *Journal of Petrology* 46, 1585–1600.
- Holness, M.B., Nielson, T.F.D., Tegner, C., 2007. Textural maturity of cumulates: a record of chamber filling, liquidus assemblage, cooling rate and large-scale convection in mafic layered intrusions. *Journal of Petrology* 48, 253–270.
- Housden, J., O'Reilly, W., Day, S.J., 1996. Variations in magnetic properties of Unit 10, Eastern Layered Intrusion, Isle of Rhum, Scotland: implications for patterns of high temperature hydrothermal alteration. *Transactions of the Royal Society of Edinburgh. Earth Sciences* 86, 91–112.
- Irvine, T.N., 1980. Magmatic density currents and cumulus processes. *American Journal of Science* 280A, 1–58.
- Irvine, T.N., Anderson, J.C., Brooks, C.K., 1998. Included blocks (and blocks within blocks) in the Skaergaard intrusion: geologic relations and the origins of rhythmic modally graded layers. *Geological Society of America Bulletin* 110, 1398–1447.
- Jackson, E.D., 1961. Primary textures and mineral associations in the ultramafic zone of the Stillwater Complex, Montana. U.S. Geological Survey Professional Paper 358 (106 pp).
- Jelinek, V., 1978. Statistical processing of anisotropy of magnetic susceptibility measured on groups of specimens. *Studia Geophysica et Geodaetica* 22, 50–62.
- Jelinek, V., 1981. Characterization of the magnetic fabric of rocks. *Tectonophysics* 79, T63–T67.
- Judd, J.W., 1885. On the Tertiary and older peridotites of Scotland. *Quarterly Journal of the Geological Society of London* 41, 354–418.
- Lagroix, F., Borradaile, G.J., 2000. Magnetic fabric interpretation complicated by inclusions in mafic silicates. *Tectonophysics* 325, 207–225.
- Lo Ré, F.C., Cheadle, M.J., Swapp, S.M., Coogan, L.A., 2003. Sedimentation in magma chambers: Evidence from the geochemistry, microstructure and crystallography of troctolite and gabbro cumulates, Rhum Layered Intrusion, Scotland EOS, *Transactions AGU* 84 (46) (Fall Meeting, Supplement, Abstract V12A-0558).
- McBirney, A.R., Nicolas, A., 1997. The Skaergaard Layered Series: Part III. Dynamic layering. *Journal of Petrology* 38, 569–580.
- McBirney, A.R., Noyes, R.M., 1979. Crystallisation and layering in the Skaergaard intrusion. *Journal of Petrology* 38, 487–554.
- Meurer, W.P., Boudreau, A.E., 1998. Compaction of igneous cumulates: Part II. Compaction and the development of igneous foliations. *Journal of Geology* 106, 293–304.
- Moseley, D., 1984. Symplectic exsolution in olivine. *American Mineralogist* 69, 139–153.
- Nicolas, A., 1992. Kinematics in magmatic rocks with special reference to gabbros. *Journal of Petrology* 33, 891–915.
- O'Driscoll, B., Donaldson, C.H., Troll, V.R., Jerram, D.A., Emeléus, C.H., 2007. An origin for harrisitic and granular olivine from the Rhum Layered Suite, NW Scotland: A crystal size distribution study. *Journal of Petrology* 48, 253–270.
- Putnis, A., 1979. Electron petrography of high-temperature oxidation in olivine from the Rhum layered intrusion. *Mineralogical Magazine* 43, 293–297.
- Renner, R., Palacz, Z.A., 1987. Basaltic replenishment of the Rhum magma chamber: evidence from Unit 14. *Journal of the Geological Society of London* 144, 961–970.
- Rochette, P., 1987. Magnetic susceptibility of the rock matrix related to magnetic fabric studies. *Journal of Structural Geology* 9 (8), 1015–1020.
- Rochette, P., Jackson, M., Aubourg, C., 1992. Rock magnetism and the interpretation of anisotropy of magnetic susceptibility. *Reviews in Geophysics* 30, 209–226.
- Rust, B.R., 1972. Pebble orientation in fluvial sediments. *Journal of Sedimentary Petrology* 42, 384–388.
- Tarling, D.H., Hrouda, F., 1993. *The Magnetic Anisotropy of Rocks*. Chapman and Hall, London.
- Tepley, F.J., Davidson, J.P., 2003. Mineral-scale Sr-isotope constraints on magma evolution and chamber dynamics in the Rhum layered intrusion, Scotland. *Contributions to Mineralogy and Petrology* 145, 628–641.

- Volker, J.A., Upton, B.G.J., 1990. The structure and petrogenesis of the Trallval and Ruinsival areas of the Rhum ultrabasic complex. *Transactions of the Royal Society of Edinburgh. Earth Sciences* 81, 69–88.
- Volker, J.A., Upton, B.G.J., 1991. Reply to comments. In: Bedard, J.H., Sparks, R.S.J. (Eds.), *Transactions of the Royal Society of Edinburgh. Earth Sciences*, vol. 82, p. 391.
- Wager, L.R., Brown, G.M., 1968. *Layered Igneous Rocks*. Oliver and Boyd, Edinburgh.
- Worrell, L.M., 2002. The origin of igneous cumulates: integrated studies of peridotites from the Western Layered Series of the Rum Layered Intrusion. Unpublished Ph.D. thesis, University of Liverpool.
- Young, I.M., Greenwood, R.C., Donaldson, C.H., 1988. Formation of the Eastern Layered Series of the Rhum Complex, northwest Scotland. *Canadian Mineralogist* 26, 225–233.